

Studies of Corrosion of Aluminium and 6063 Aluminium Alloy in Phosphoric Acid Medium

Deepa Prabhu, Padmalatha*,

**Department of Chemistry, Manipal Institute of Technology, Manipal University,
Karnataka 576104, India**

***Corres.author: drpadmalatharao@yahoo.com**

Abstract: The corrosion behaviour of aluminium and 6063 aluminium alloy was investigated in phosphoric acid of different concentrations at different temperatures. The study was done by electrochemical method, using Tafel polarization and electrochemical impedance spectroscopy (EIS) techniques. The kinetic parameters and thermodynamic parameters were calculated using Arrhenius theory and transition state theory. The surface morphology was studied using scanning electron microscope (SEM) with Energy dispersive X-ray (EDX). The corrosion rate of both the materials increased with increase in the concentration of acid as well as with temperature. The rate of corrosion of 6063 aluminium alloy was found to be higher than that of pure aluminium. Suitable mechanism was proposed for the corrosion of aluminium and 6063 aluminium alloy in phosphoric acid medium. The results obtained by Tafel polarization and electrochemical impedance spectroscopy (EIS) techniques were in good agreement with each other.

Keywords: Aluminium, 6063 aluminium alloy, phosphoric acid, Tafel polarization, EIS technique, SEM-EDX.

1. Introduction

Corrosion, which is an inevitable problem faced in almost all industries can be considered as one of the worst technical calamity of our time. Besides from its direct loss in dollars, corrosion is a serious problem because it definitely contributes to the depletion of our natural resources. Corrosion studies have also become important due to increasing awareness of the need to conserve the world's metal resources [1]. Now-a-days more attention has been paid to control the metallic corrosion, due to increasing use of metals in all fields of technology.

Corrosion studies of aluminium and aluminium alloys have received considerable attention by researchers because of their technological importance and industrial applications. Aluminium is second to iron in terms of production and consumption. Aluminium and aluminium alloys find applications, mainly in automobiles, aviation, household appliances, containers and electronic devices [2-5].

Aluminium and aluminium alloys have emerged as alternate materials in aerospace and in some chemical processing industries. Aluminium and aluminium alloys find vast applications because of the natural tendency of aluminium to form a passivating oxide layer. However, in the aggressive corrosive environment the protective layer breaks down, and the material will undergo corrosion. Reported literature reveals that extensive studies are conducted on corrosion behaviour of aluminium and aluminium alloys in hydrochloric acid and sulphuric acid medium [6-10].

Phosphoric acid is a major industrial chemical, which is widely used for acid cleaning and electropolishing of aluminium [11]. Even though dissolution rate of aluminium in phosphoric acid is lower,

compared to the dissolution of the same in hydrochloric or sulphuric acid, it does corrode aluminium and its alloys. Phosphoric acid is also used in pickling delicate, costly components and precision items where rerusting after pickling has to be avoided.

According to the available literature, not much study has been done regarding the corrosion behaviour of aluminium and 6063 aluminium alloy in phosphoric acid medium. As part of our studies with corrosion behaviour of aluminium and aluminium alloys in different media and corrosion control of the same using green inhibitors [12]. We report herein the results of corrosion behaviour of aluminium and 6063 aluminium alloy in phosphoric acid medium of different concentrations at different temperatures.

2. Experimental

2.1 Material

The experiments were performed with specimens of aluminium and 6063 aluminium alloy. The composition of aluminium and 6063 aluminium alloy specimen is given in the Table 1.

Table 1. Composition of the pure aluminium (99.6%) and 6063 aluminium alloy specimen (% by weight)

Element	Composition (%)	
	Pure aluminium	6063 aluminium alloy
Si	0.120	0.412
Fe	0.270	0.118
Cu	-	0.0570
Mg	-	0.492
Al	Balance	Balance

2.2 Preparation of Test coupons

Cylindrical test coupons were sealed with Acrylic resin material in such a way that the area exposed to the medium was 0.7cm² of aluminium and 1.0 cm² of 6063 aluminium alloy. It was polished with different grade emery papers. Further polishing was done with disc polisher using levigated alumina to get mirror surface. It was then dried and stored in a desiccator to avoid moisture before used for corrosion studies.

2.3 Preparation of Medium

A stock solution of phosphoric acid was prepared using analytical grade phosphoric acid (85%) and double distilled water. It was standardized by potentiometric method. Phosphoric acid solutions of required concentrations were prepared by appropriate dilution. Experiments were carried out using a calibrated thermostat at temperature range of 30°C - 50°C ($\pm 0.5^\circ\text{C}$).

2.4 Electrochemical measurements

Electrochemical measurements were carried out by using an electrochemical work station, (CH600D-series, U.S. Model with CH instrument beta software). The electrochemical cell used was a conventional three-electrode compartment having glass cell with a platinum counter electrode and a saturated calomel electrode (SCE) as reference. The working electrode was made up of aluminium and 6063 aluminium. All the values of potential were measured with reference to the saturated calomel electrode. The polarization studies were done immediately after the EIS studies on the same electrode without any further surface treatment.

2.4 (a) Tafel polarization studies

Finely polished specimens with 0.7cm² and 1 cm² surface area were exposed to corrosion medium of different concentrations phosphoric acid (2.0 M, 1.0M, and 0.5M) at temperature range of 30°C to 50°C. The

potentiodynamic current-potential curves were recorded by polarizing the specimen to -250 mV cathodically and $+250$ mV anodically with respect to open circuit potential (OCP) at a scan rate of 0.01 V/s.

2.4(b) Electrochemical impedance spectroscopy (EIS) studies

Electrochemical impedance spectroscopy (EIS) measurements were carried out using a small amplitude ac signal of 10 mV over a frequency range of 100 kHz- 0.01 Hz. The charge transfer resistance R_{ct} was obtained from Nyquist plot. The values of R_{ct} is inversely proportional to the corrosion rate [13].

2.5 Scanning electron microscopy (SEM) and Energy-dispersive X-ray spectroscopy (EDX) studies

The scanning electron microscope images were recorded to establish the interaction of acid medium with the metal surface using EVO 18-15-57 scanning electron microscope with Energy-dispersive X-ray spectroscopy. The surface morphology of aluminium and 6063 aluminium alloy immersed in phosphoric acid was compared with that of uncorroded sample.

3. Results And Discussion

3.1 Electrochemical measurements

3.1(a) Tafel polarization measurements

The effect of phosphoric acid concentrations on the corrosion rate of aluminium and 6063 aluminium alloy sample was studied using Tafel polarization technique. Figure 1 and Figure 2 represents the potentiodynamic polarization curves of aluminium and 6063 aluminium alloy in different phosphoric acid solutions at 30°C respectively.

The potentiodynamic polarization parameters like corrosion potential (E_{corr}), corrosion current density (i_{corr}), anodic and cathodic slopes (b_a and b_c) are obtained from the polarization studies. The corrosion rate was calculated using equation (1)

$$\hat{r}_{\text{corr}} \left(\text{mm y}^{-1} \right) = \frac{3270 \times M \times i_{\text{corr}}}{\dots \times Z} \quad (1)$$

Where 3270 is a constant that defines the unit of corrosion rate, i_{corr} is the corrosion current density in A cm^{-2} , is the density of the corroding material (g cm^{-3}), M is the atomic mass of the metal, and Z is the number of electrons transferred per atom. [14]. The results of Tafel polarization measurements are reported in the Table 2 and Table 3 respectively.

As can be seen from Figure 1 and Figure 2, the corrosion potential is shifted in the positive direction, when the concentration of the acid is increased. The positive shift in the corrosion potential E_{corr} with the increase in the concentration of acid indicate that the anodic process is much more affected than the cathodic process [15]. This observation is in accordance with Murrallidharan [16], who proposed dependence of E_{corr} and i_{corr} on solution parameters. Tafel slopes remained almost unchanged indicating that acid strength do not change the mechanism of the corrosion process.

It is evident from data of Table 2 and Table 3, corrosion rate is more in case of 6063 aluminium alloy than that of pure aluminium. The increased corrosion resistance of pure aluminium is mainly attributed towards the formation of stable oxide layer on its surface. As seen from Table 1, in case of 6063 aluminium alloy there is influence of both Silicon and Magnesium. The addition of these alloying elements could lead to the discontinuities on the oxide film, thereby increasing the number of sites where corrosion can be initiated. This makes 6063 aluminium to undergo corrosion at a faster rate [17, 18].

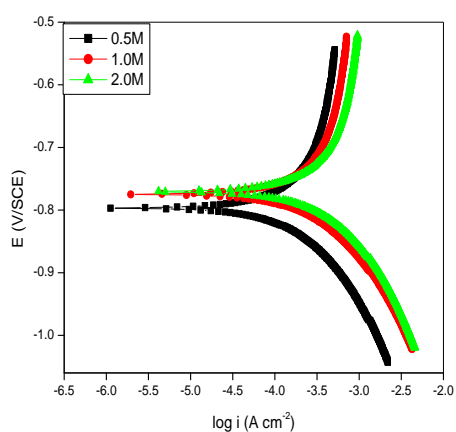


Fig.1. Tafel polarization curves for pure aluminium in different concentrations of phosphoric acid solutions at 30°C

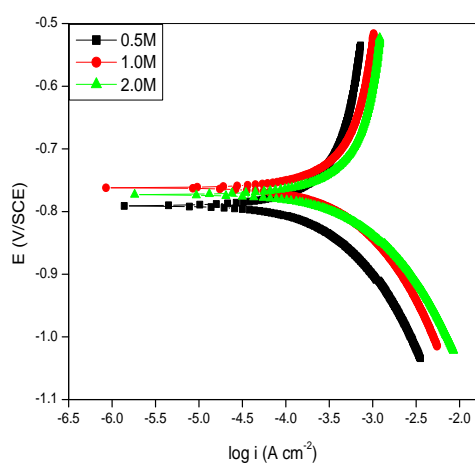


Fig. 2. Tafel polarization curves for 6063 aluminium alloy in different concentrations of phosphoric acid solutions at 30°C

Table 2. Results of Tafel polarization studies of aluminium in phosphoric acid solutions

[H ₃ PO ₄] M	Temp °C	E _{corr} (mV vs SCE)	i _{corr} (×10 ⁻⁵ A cm ⁻²)	ba (mVdec ⁻¹)	-bc (mVdec ⁻¹)	C.R (mm y ⁻¹)
0.5	30	-797	17.34	354	637	1.89
	35	-793	21.91	353	610	2.38
	40	-797	27.56	364	596	3.00
	45	-804	40.21	367	595	4.38
	50	-800	47.75	379	579	5.20
1.0	30	-783	25.87	336	674	2.81
	35	-790	30.12	348	680	3.28
	40	-794	41.11	353	658	4.48
	45	-796	55.37	358	620	6.03
	50	-805	75.79	363	589	8.26
2.0	30	-770	36.85	336	660	4.01
	35	-769	48.48	329	702	5.28
	40	-766	63.59	334	646	6.93
	45	-773	93.98	339	623	10.24
	50	-782	110.7	364	588	12.06

Table 3.Results of Tafel polarization studies of 6063 aluminium alloy in phosphoric acid solutions

[H ₃ PO ₄] M	Temp °C	E _{corr} (mV vs SCE)	i _{corr} (×10 ⁻⁵ A cm ⁻²)	ba (mV dec ⁻¹)	-bc (mV dec ⁻¹)	C.R (mm y ⁻¹)
0.5	30	-791	24.6	350	675	2.68
	35	-794	29.9	355	691	3.25
	40	-805	42.0	360	658	4.57
	45	-817	56.9	378	612	6.20
	50	-826	74.9	388	569	8.16
1.0	30	-762	38.6	334	672	4.20
	35	-778	50.5	343	658	5.50
	40	-788	69.2	350	643	7.54
	45	-805	96.0	369	597	10.46
	50	-809	135.4	379	560	14.75
2.0	30	-773	44.85	335	733	4.88
	35	-771	57.61	337	698	6.27
	40	-779	86.41	344	645	9.41
	45	-775	111.0	379	564	12.09
	50	-794	192.4	349	537	20.97

3.1 (b) Electrochemical impedance measurements

The corrosion behaviour of aluminium and 6063 aluminium alloy specimens was also investigated by EIS in various concentrations of phosphoric acid. The impedance spectra are recorded and displayed as Nyquist plots as a function of acid strength. Nyquist plots for different concentrations of phosphoric acid are shown in the Figure 3 and 4 respectively.

From Figure 3 it is obvious that, the impedance diagrams show semicircles, indicating that the corrosion process is mainly charge transfer controlled [18, 19]. The general shape of the curve is similar for all individual samples of the alloy, with large capacitive loop at high frequencies (HF) and an inductive loop at low frequencies (LF). Similar impedance plots have been reported in literature for the corrosion of aluminium and aluminium alloys in various electrolytes such as, sodium sulphate [20], sulphuric acid [21] etc. The HF capacitive loop is attributed to the presence of a protective oxide film covering the surface of the metal. According to Brett [22, 23], the capacitive loop is corresponding to the interfacial reactions, particularly, the reaction of aluminium oxidation at the metal/oxide/electrolyte interface. The process includes the formation of Al⁺ ions at the metal/oxide interface, and their migration through the oxide/solution interface where they are oxidized to Al³⁺. At the oxide/solution interface, OH⁻ or O²⁻ ions are also formed. The fact that all the three processes are represented by only one loop could be attributed either to the overlapping of the loops of processes, or to the assumption that one process dominates and, therefore, excludes the other processes [24]. The other explanation offered to the high frequency capacitive loop is the oxide film itself. The origin of the inductive loop has often been attributed to surface or bulk relaxation of species in the oxide layer [25]. The LF inductive loop may be related to the relaxation process obtained by adsorption and incorporation of phosphate ions on and into the oxide film [26].

The depressed semicircles of the Nyquist plots suggest the distribution of capacitance due to inhomogeneities associated with the electrode surface [27]. The EIS results are reported in Table 4 and Table 5.

An equivalent circuit of nine elements depicted in Figure 5a was used to simulate the measured impedance data, as shown in Figure 5b. In this equivalent circuit R_s is the solution resistance and R_{ct} is the charge transfer resistance. R_L and L represent the inductive elements. This also consists of constant phase element; CPE (Q) in parallel to the series capacitors C₁, C₂ and series resistors R₁, R₂, R_L and R_{ct}. R_L is parallel with the inductor L. The polarization resistance R_p and double layer capacitance C_{dl} can be calculated from equations (2) and (3):

$$R_p = R_L + R_{ct} + R_1 + R_2 \tag{2}$$

$$C_{dl} = C_1 + C_2 \tag{3}$$

It was observed that the value of CPE decreases while the value of R_p increases with increasing concentration of acid mixture. The measured value of polarization resistance increases while the CPE value decreases with increasing concentration of the acid, indicating that the rate of corrosion increases with increase in concentration of acid solution. This is in agreement with the results obtained from potentiodynamic polarization data.

The corrosion current density i_{corr} is calculated using the charge transfer resistance value, R_{ct} , using with the Stern–Geary equation (4)

$$i_{corr} = \frac{b_a b_c}{2.303 (b_a + b_c) R_{ct}} \tag{4}$$

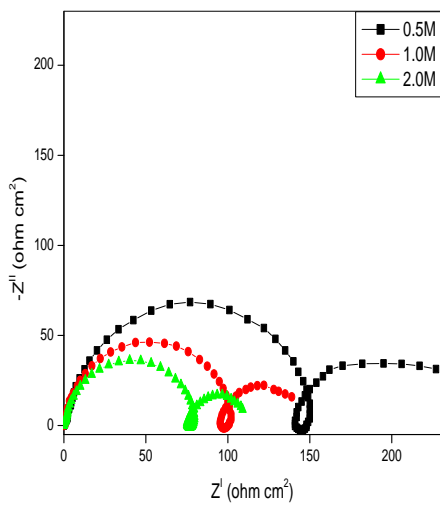


Fig. 3. Nyquist Plot for aluminium in different concentrations of phosphoric acid solutions at 30°C

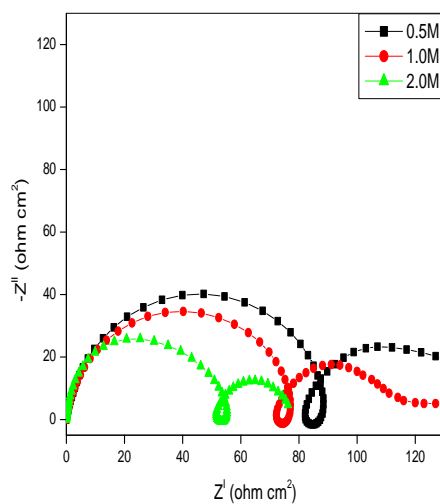


Fig. 4. Nyquist Plot for 6063 aluminium alloy in different concentrations of phosphoric acid solutions at 30°C

Table 4.Results of ESI studies of aluminium in phosphoric acid solution

[H ₃ PO ₄] M	Temp °C	R _p (ohm cm ²)	CPE (μ F cm ⁻²)
0.5	30	241.3	15
	35	195.9	26
	40	154.2	32
	45	102.4	46
	50	85	58
1.0	30	156.3	38
	35	130.2	45
	40	94.5	58
	45	70.2	66
	50	50.2	75
2.0	30	108.3	66
	35	76.9	82
	40	59.7	110
	45	38.0	125
	50	31.2	146

Table 5: Results of ESI studies of 6063 aluminium alloy in phosphoric acid solution

Molarity of H ₃ PO ₄	Temp °C	R _p (ohm cm ²)	CPE (μ F cm ⁻²)
0.5	30	162.2	30
	35	128.8	51
	40	91.5	62
	45	67.1	92
	50	50.5	116
1.0	30	101.70	69
	35	75.90	78
	40	54.00	90
	45	36.80	117
	50	24.20	129
2.0	30	80.7	130
	35	62.9	165
	40	40.8	221
	45	31.5	251
	323	15.5	290

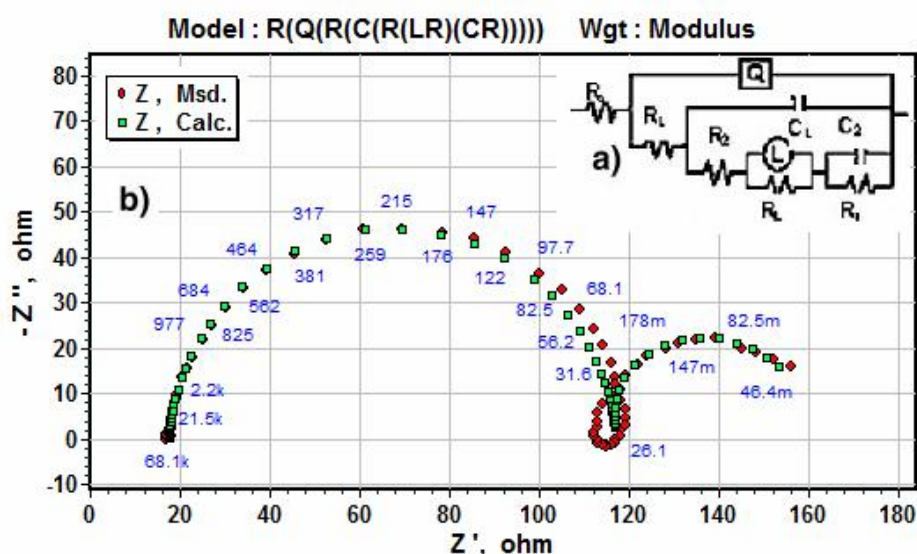


Fig. 5. Equivalent circuit fit for pure aluminium in 1M phosphoric acid solution at 30°C

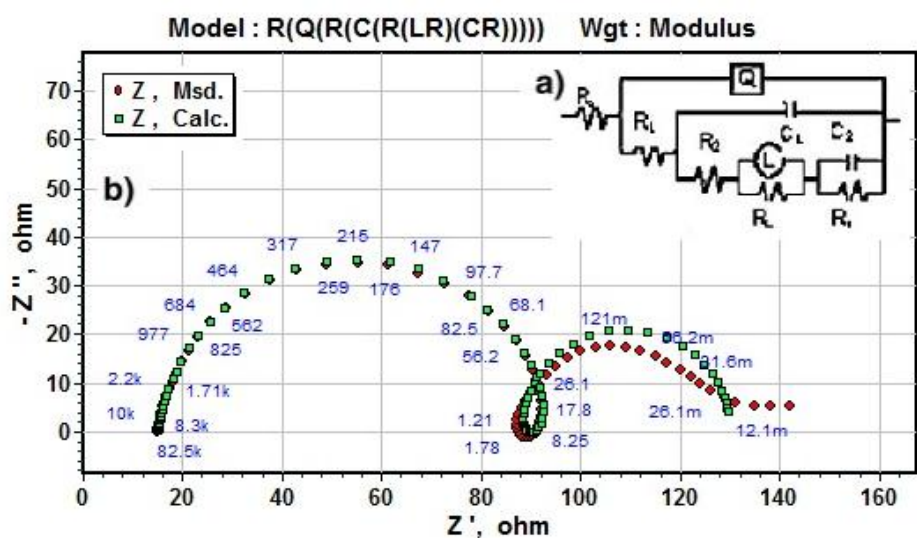


Fig. 6. Equivalent circuit fit for 6063 aluminium alloy in 1M phosphoric acid solution at 30°C

3.2 Effect of temperature

Temperature is an important parameter in studies on material corrosion. The dependence of temperature on corrosion rate reveals valuable thermodynamic parameters like energy of activation, enthalpy of activation and entropy of activation for the corrosion process. The effect of temperature on the corrosion rate of the aluminium and 6063 alloy was studied by measuring the corrosion rate at the temperature range of 30°C to 50°C. Figure 7 and Figure 8 represents the potentiodynamic polarization curves of aluminium and 6063 aluminium alloy in 1M phosphoric acid solution at temperature range of 30°C to 50°C. Figure 9 and Figure 10 represents Nyquist plots for the same.

From both measurements it is obvious that the corrosion rate increased with increase in temperature. This is because the hydrogen evolution overpotential decreases with increase in the temperature [28]. Further, with increase in temperature, the naturally occurring oxide film becomes thin, porous and less protective. This results in the rapid dissolution of the oxide film, thereby enhancing the corrosion rate.

The energy of activation of corrosion of aluminium and 6063 aluminium alloy was calculated from Arrhenius equation (5). The Arrhenius plot ($\ln CR$ vs $1/T$) at all the concentrations of phosphoric acid is represented in the Figure 11 and Figure 12.

$$\ln(CR) = B - \frac{E_a}{RT} \quad (5)$$

Where B is a constant, R is the universal gas constant, and T is the absolute temperature.

Enthalpy of activation (H_a) and entropy of activation (S_a) were calculated from the transition state theory equation (6),

$$CR = \frac{RT}{Nh} \exp\left(\frac{S_a}{R}\right) \exp\left(\frac{H_a}{RT}\right) \quad (6)$$

Where h is Planck's constant and N is Avagadro's number. A plot of $\ln(CR/T)$ vs $1/T$ gave a straight line with slope $= -H_a/T$ and intercept $= \ln(R/Nh) + S_a/R$. The plots of $\ln(CR/T)$ vs $1/T$ for the corrosion of aluminium and 6063 aluminium alloy in the presence of different concentrations phosphoric acid is shown in Figure 13 and Figure 14.

The values of energies of activation, enthalpy of activation and entropy of activation are listed in Table 6. As indicated in Table 6, value of energy of activation is greater than 20 kJ mol^{-1} both for aluminium and 6063 aluminium alloy. This suggested that the whole process is controlled by surface reaction [29]. This phenomenon may be due to the fact that the activation energy for the corrosion reaction is independent of concentration polarization and mainly due to activation polarization.

The entropy of activation is large and negative. This implies that the activated complex in the rate determining step represents association rather than dissociation, indicating that a decrease in disorder takes place, in going from reactant to the activated complex [30]. The value of ΔS_a increased with increase in acid concentration reveals that dissolution of alloy is facilitated as the concentration of the acid medium increases.

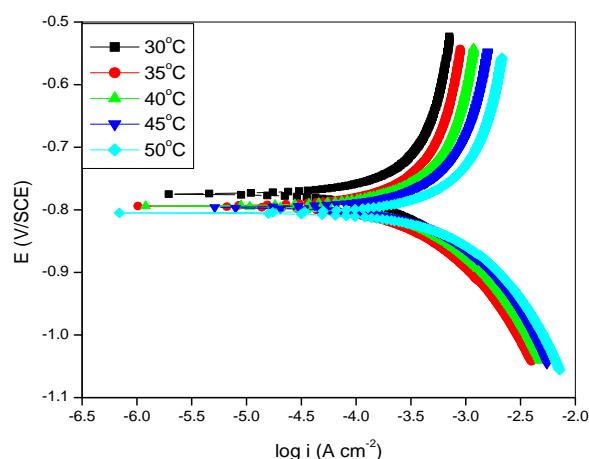


Fig. 7. Tafel polarization curves for pure aluminium at different temperatures in 1M phosphoric acid solution

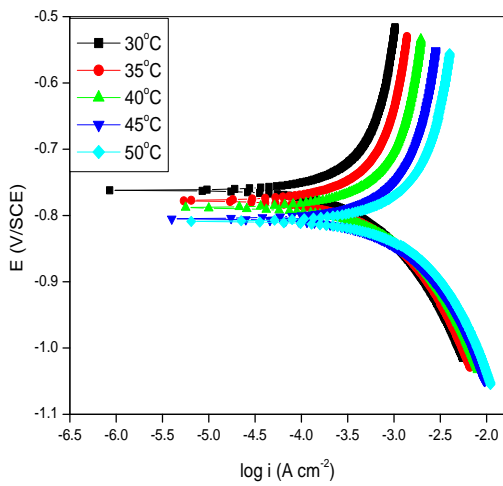


Fig. 8.Tafel polarization curves for 6063 aluminium alloy at different temperatures in 1M phosphoric acid solution

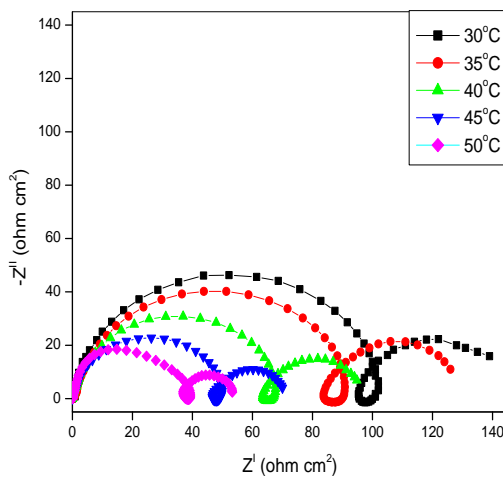


Figure 9: Nyquist plots for the corrosion of aluminium at different temperature in 1M phosphoric acid solution

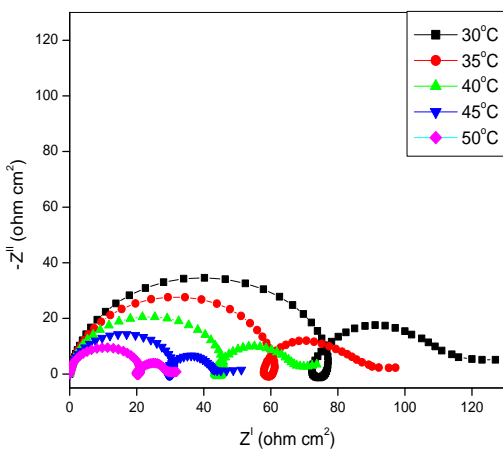


Figure 10:Nyquist plots for the corrosion of 6063 aluminium alloy at different temperature in 1M phosphoric acid solution

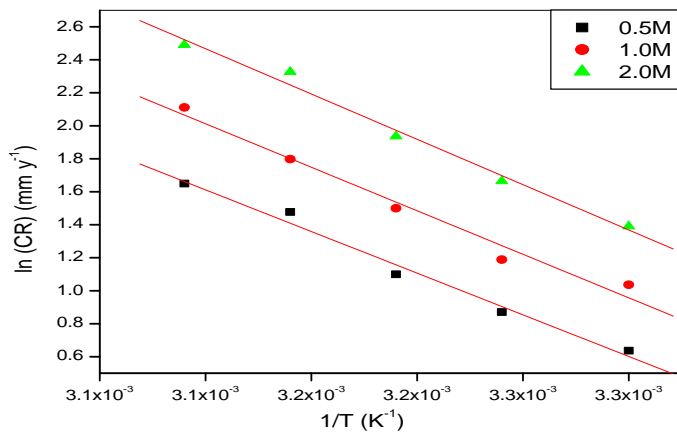


Fig. 11. Arrhenius plots for the corrosion of pure aluminium in phosphoric acid solution

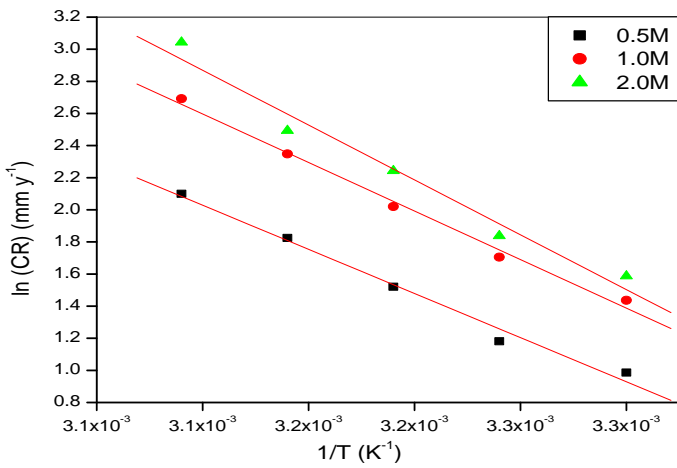


Fig. 12. Arrhenius plots for the corrosion of 6063 aluminium alloy in phosphoric acid solution

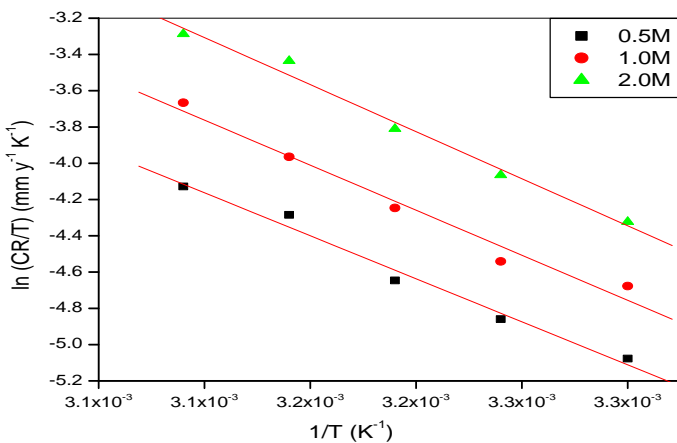


Fig. 13. Plots of $\ln(CR/T)$ vs $1/T$ for the corrosion of aluminium in phosphoric acid solutions

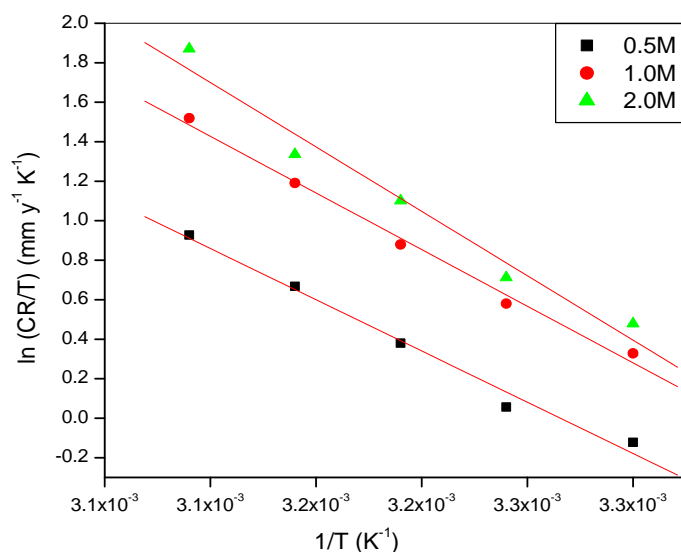


Fig. 14. Plots of $\ln(CR/T)$ vs $1/T$ for the corrosion of 6063 aluminium alloy in phosphoric acid solution.

Table 6: Activation parameters for the corrosion of aluminium and 6063 aluminium in phosphoric acid solutions

H_3PO_4 (M)	E_a (kJ mol ⁻¹)		H_a (kJ mol ⁻¹)		S_a (J mol ⁻¹ K ⁻¹)	
	Pure	Alloy	Pure	Alloy	Pure	Alloy
0.5	45.707	41.9868	43.155	39.4350	-56.645	-109.934
1.0	50.244	43.852	47.692	41.3002	-37.858	-100.821
2.0	56.784	45.6857	54.2321	43.1339	-15.3207	-91.353

3.3 SEM-EDX Studies

The SEM images of freshly polished surface of aluminium and 6063 aluminium alloy is given in Figure 15(a) and Figure 16(a) which show un-corroded surface with few scratches due to polishing. The surface morphology of the aluminium and 6063 aluminium alloy sample was examined by SEM immediately after corrosion tests in 1.0M phosphoric acid medium. The SEM image of corroded sample of aluminium is in Figure 15b. Figure 16b shows degradation of alloy.

For aluminium there is deposition of aluminium phosphate precipitate on the surface and for 6063 aluminium alloy due to the alloying elements, it may be attributed to deposition of the phase Mg_5Al_8 which makes an anodic phase in the aluminium matrix and Si act as cathode and contribute to the intergranular corrosion and resulting in uniform attack and making it an optimum region of dissolution [31]. Close observation of SEM metals images indicates the deposition of precipitates of aluminium phosphate on the surface aluminium and magnesium phosphate on 6063 aluminium alloy.

Figure 17a and Figure 18a represents EDX spectrum of the uncorroded sample of aluminium and 6063 aluminium alloy. The spectrum shows peaks for aluminium and oxygen suggesting the presence of aluminium oxide/hydroxide. Figure 17b and Figure 18b depicts the EDX spectrum for the corroded sample of both. The presence of peak corresponding to phosphorous indicates the attack of phosphoric acid. The results of EDX analysis is reported in Table 7.

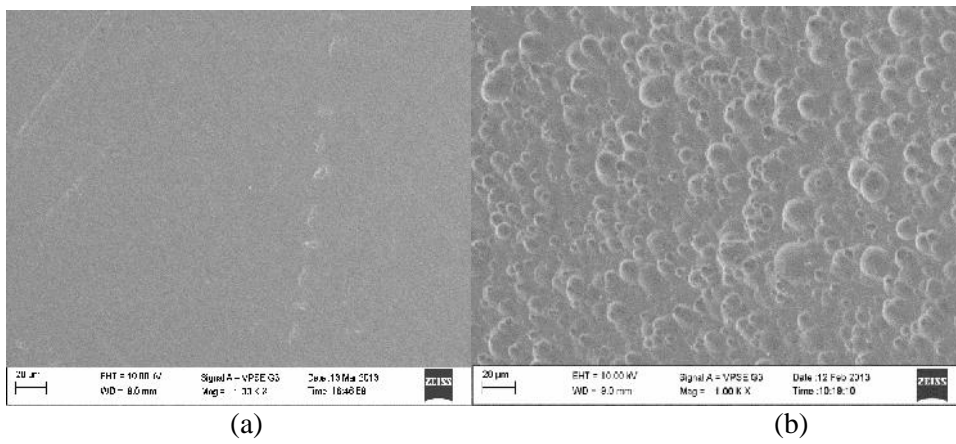


Fig. 15.SEM image of (a) freshly polished surface of the pure aluminium (b) after immersion in 1M phosphoric acid solution

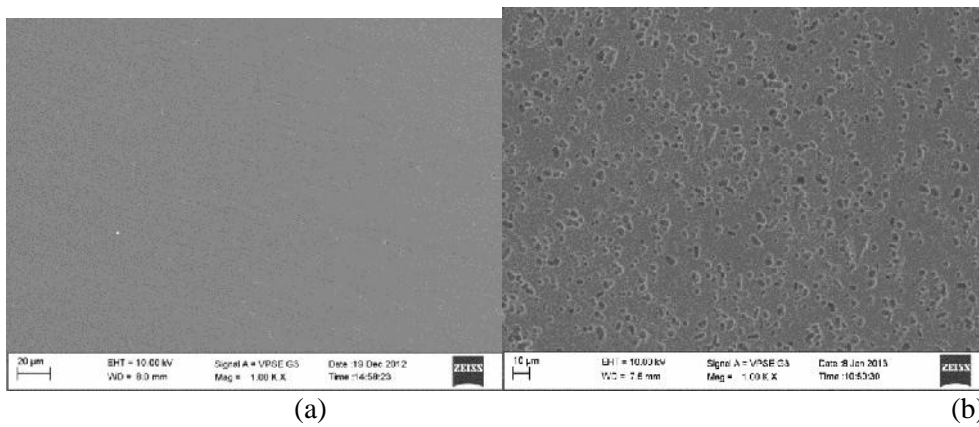


Fig. 16.SEM image of (a) freshly polished surface of 6063 aluminium alloy (b) after immersion in 1M phosphoric acid solution

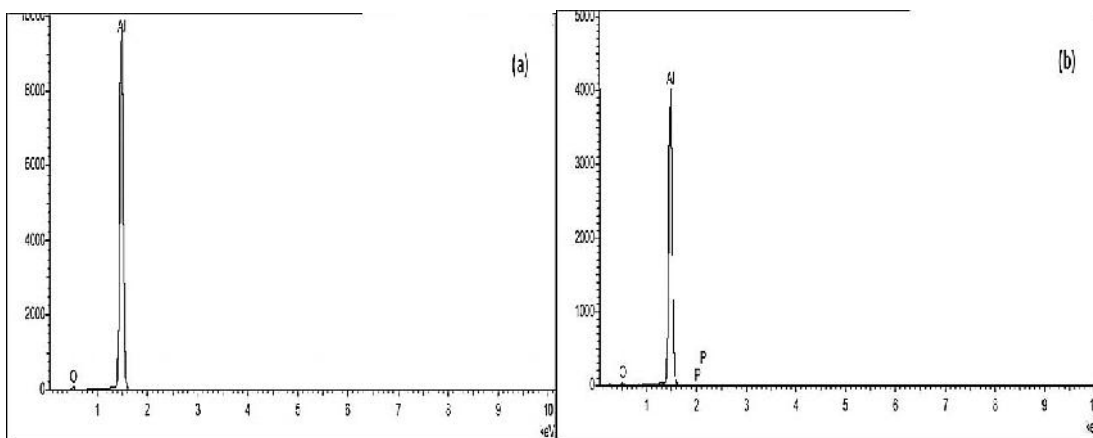


Fig. 17. SEM image of (a) freshly polished surface of the pure aluminium (b) after immersion in 1M phosphoric acid solution

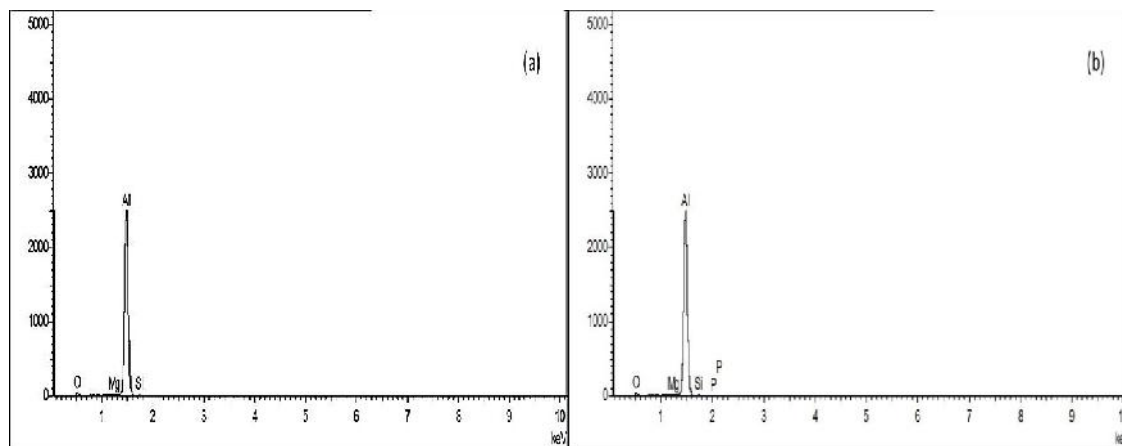


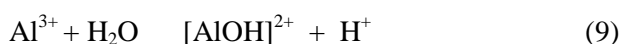
Fig.18. EDX spectrum of (a) uncorroded sample of the 6063 aluminium alloy (b) 6063 Aluminium alloy after immersion in 1M phosphoric acid solution.

Table 7 : EDX analysis result of aluminum, 6063 aluminium alloy in absence and presence of 1.0 M Phosphoric acid solution

Medium	Composition (%)				
	Al	O	Si	Mg	P
Aluminum	89.40	10.60	-	-	-
6063 aluminium alloy	94.70	4.60	0.45	0.25	-
aluminum in 1.0M phosphoric acid	84.17	14.77	-	-	1.06
6063 aluminium alloy in 1.0M phosphoric acid	94.73	4.34	0.54	0.30	0.09

3.4 Mechanism of corrosion process

Aluminium and its alloys have air formed oxide film of amorphous alumina which initially thickens on exposure to neutral aqueous solution with the formation of a layer of crystalline hydrated alumina [32]. In acidic solutions the anodic process of corrosion is the dissolution [33] of the metal ions from the oxide free metal surface into the solution.



The principal cathodic process is the discharge of hydrogen ions to produce hydrogen gas.



4. Conclusions

- Pure aluminium undergoes less corrosion in phosphoric acid medium when compared with 6063 aluminium alloy.
- The corrosion rate increases with increase in the concentration of phosphoric acid.
- The corrosion rate increases with increase in temperature in both metals.
- The results of Tafel polarization and EIS studies are in good agreement with one another.

Acknowledgement

Mrs. Deepa Prabhu, acknowledges Manipal University, for the Fellowship, and chemistry department MIT Manipal, for laboratory facilities.

References

1. Stansbury E.E and Buchanan R.A., Fundamentals of Electrochemical Corrosion ASM. International Materials Park, USA, 2000.
2. Christian Vargel Corrosion of aluminium Elsevier Ltd. New York, 2004.
3. Kosting P.R and Heins C., Corrosion of metals by phosphoric acid. Ind. Eng. Chem., 1931, 23, 140-150.
4. Badaway W.A, Alkharafi F.M, and El-Azab A.S., Electrochemical behavior and corrosion inhibition of Al, Al-6061 and Al-Cu in neutral aqueous solutions. Corro. Sci., 1999, 41, 709-727.
5. Desai P.S and Kapopara S.M., Inhibiting effect of anisidines on corrosion of aluminium in hydrochloric acid. Ind. J. Chem. Tech., 2009, 16, 486-491.
6. Paul and Sigwalt Juniere M., Aluminium in the Chemistry and Food Industries. British Aluminium Co. Ltd. London, 1964, 46.
7. Ating E.I., Umoren S.A., Udousoro I.I., Ebenso E.E. and Udoh A.P., Leaves extract of *Ananassativum* as green corrosion inhibitor for aluminium in hydrochloric acid solutions. Green Chemistry Letters and Reviews, 2010, 3, 61-68.
8. Umoren S.A., Obot I.B., Ebenso E.E., and Obi-Egbedi N.O., The Inhibition of aluminum corrosion in hydrochloric acid solution by exudate gum from *Raphiahookeri*. Desalination, 2009, 247, 561-572.
9. Obi-Egbedi N.O., Obot I.B., and Umoren S.A., *Spondiasmombin* L. as a green corrosion inhibitor for aluminium in sulphuric acid: Correlation between inhibitive effect and electronic properties of extracts major constituents using density functional theory. Arabian Journal of Chemistry, 2012, 5, 361-373.
10. Nnanna L.A., Anozie I.U., Avoaja A.G.I., Akoma C.S. and Eti E.P., Comparative study of corrosion inhibition of aluminium alloy of type AA3003 in acidic and alkaline media by *Euphorbia hirta* extract. African Journal of Pure and Applied Chemistry, 2011, 5, 265-271.
11. Amin Mohammed A., Mohsen Q., Omar Hazzazi A., Synergistic effect of Γ ions on the corrosion inhibition of Al in 1.0 M phosphoric acid solutions by purine. Mater. Chem Phys., 2009, 114, 908-914.
12. Deepa Prabhu and Padmalatha Rao, Corrosion inhibition of 6063 aluminum alloy by *Coriandrumsativum* L seed extract in phosphoric acid medium. J. Mater. Environ. Sci., 2013, 4, 732-743.
13. Poorqasemi E., Abootalebi O., Peikari M., and Haqdar F., Investigating accuracy of the Tafel extrapolation method in HCl solutions. Corros. Sci., 2009, 51, 1043-1054.
14. Fontana M.G., Corrosion Engineering, 3rd edn, McGraw-Hill, Singapore, 1987.
15. El-Sayed, Phenothiazine as inhibitor of the corrosion of cadmium in acidic solutions. J. Appl. Electrochem., 1997, 27, 193-200.
16. Muralidharan V.S. and Rajagopalan K.S., Kinetics and mechanism of corrosion of iron in phosphoric acid. Corros. Sci., 1979, 19, 205-207.

17. Pardo A., Merino M.C., Merino S., Lopez M.D., Viejo F., Carboneras M., Influence of reinforcement grade and matrix composition on corrosion resistance of cast aluminium matrix composites (A3xx.x/SiCp) in a humid environment. *Mater. Corros.*, 2003, 54, 311-317.
18. Trowsdale A.J., Noble B., Harris S.J, Gibbins I.S.R., Thompson G.E. and Wood G.C., The influence of silicon carbide reinforcement on the pitting behaviour of aluminium. *Corros. Sci.*, 1996, 2, 177-191.
19. Montecelli C., Zucchi F., Brunoro G and Trabanelli G., Corrosion and corrosion inhibition of alumina particulate/aluminium alloys metal matrix composites in neutral chloride solutions. *J. Appl. Electrochem.*, 1997, 27, 325-334.
20. Sayed S., Abdel Rehim, Hamdi Hassan H and Mohammed Amin A., Corrosion and corrosion inhibition of Al and some alloys in sulphate solutions containing halide ions investigated by an impedance technique. *Appl. Surf. Sci.*, 2002, 187, 279-290.
21. Lenderink H.J.W., Linden M.V.D and De Wit J.H.W., Corrosion of aluminium in acidic and neutral solutions. *Electrochim Acta*, 1993, 38, 1989-1992.
22. Brett C.M.A., The application of electrochemical impedance techniques to aluminium corrosion in acidic chloride solution. *J. Appl. Electrochem.* 1990, 20, 1000-1003.
23. Brett C.M.A., On the electrochemical behaviour of aluminium in acidic chloride solution. *Corro. Sci.*, 1992, 33, 203-210.
24. Wit J.H. and Lenderink H.J.W., Electrochemical impedance spectroscopy as a tool to obtain mechanistic information on the passive behaviour of aluminium. *Electrochim. Acta.*, 1996, 41, 1111-1119.
25. Frers S.E., Stefanel M.M., Mayer C. and Chierchie T., AC-Impedance measurements on aluminium in chloride containing solutions and below the pitting potential. *J. Appl. Electrochem.*, 1990, 20, 996-999.
26. Lorenz W.J and Mansfeld F. Determination of corrosion rates by electrochemical DC and AC methods. *Corros. Sci.*, 1981, 21, 647-672.
27. El Hosary A.A., Saleh R.M. and Shams El Din A.M., Corrosion inhibition by naturally occurring substances-I. The effect of *Hibiscus subdariffa* (karkade) extract on the dissolution of Al and Zn. *Corro. Sci.*, 1972, 12, 897-904.
28. Popova A., Sokolova E., Raicheva S., Christov M., AC and DC study of the temperature effect on mild steel corrosion in acid media in the presence of benzimidazole derivatives. *Corros. Sci.*, 2003, 45, 33-58.
29. Bouklah M., Hammouti B., and Benkaddour M., Thiophene derivatives as effective inhibitors for the corrosion of steel in 0.5 m H₂SO₄. *J. App. Electro.Chem.*, 2005, 35, 1095-1101.
30. AbdEl-Rehim S.S., Ibrahim M.A.M. and Khaled K.F., Aminoantipyrine as an inhibitor of mild steel corrosion in HCl solution. *J. Appl. Electrochem.*, 1999, 29, 593-599.
31. Scamans G.M., Jholroyd N. and Tuck C.D., The role of magnesium segregation in the intergranular stress corrosion cracking of aluminium alloys. *Corros. Sci.*, 1987, 27, 329-347.
32. Hart R.K., The formation of films on aluminium immersed in water. *Trans. Faraday Soc.*, 1957, 53, 1020-1027.
33. Obot I.B, Obi-Egbedi N.O, Umoren S.A. and Ebenso E.E., Synergistic and Antagonistic Effects of Anions and *Ipomoea invulcrata* as Green Corrosion Inhibitor for Aluminium Dissolution in Acidic Medium. *Int. J. Electrochem. Sci.*, 2010, 5, 994-1007.
